Jpn. J. Cancer Res. **92**, 959–967, September 2001

PI3-kinase p85α Is a Target Molecule of Proline-rich Antimicrobial Peptide to Suppress Proliferation of ras-Transformed Cells

Koji Tanaka,[1] Yoshinori Fujimoto,[1,2] Masako Suzuki, Yasuaki Suzuki, Takaaki Ohtake, Hiroyuki Saito and Yutaka Kohgo

Third Department of Internal Medicine, Asahikawa Medical College, 2-1 Midorigaoka-Higashi, Asahikawa 078-8510

PR-39, which is an endogenous antimicrobial peptide, can bind to Src homology 3 domains of the NADPH complex protein $p47^{phox}$ and the signaling adapter protein $p130^{Cas}$. Recently, we have reported that *PR-39* gene transduction altered invasive activity and actin structure of human hepatocellular carcinoma cells, suggesting that this peptide affects cellular signaling due to its proline-rich motif. In order to clarify the mechanism of the PR-39 functions, we transfected the *PR-39* gene into mouse NIH3T3 cells which had already been transformed with human activated *k-ras* gene. The *PR-39* gene transfectant showed a reorganization of actin structure and suppression of cell proliferation both *in vitro* and *in vivo*. Decreases of MAP (mitogen-activated protein) kinase activity, cyclin D1 expression and JNK activity were observed in the *PR-39* gene transfectant. Co-immunoprecipitation analysis revealed that PR-39 binds to PI3-kinase p85α, which is a regulatory subunit of PI3-kinase and one of the effectors by which ras induces cytoskeletal changes and stimulates mitogenesis. The PI3-kinase activity of the *PR-39* gene transfectant was decreased compared with that of the ras transformant. These results suggest that PR-39 alters actin structure and cell proliferation rate by binding to PI3-kinase p85α and suppressing the PI3-kinase activity.

Key words: PR-39 — Antimicrobial peptide — PI3 kinase — ras — Actin

PR-39 is an endogenous proline-rich antimicrobial peptide isolated from pig small intestines and neutrophils,[1,2] and has been recognized as an important mediator of innate immunity against microbes.[3] In addition to bactericidal activity, this peptide has multiple biological functions including wound repairing,[4] angiogenesis,[5] and inhibition of tumor cell invasion.[6] PR-39 is secreted as a prepropeptide that includes a canonical leader sequence, and rapidly undergoes cleavage of the N-terminal portion to generate the mature form composed of the 39 C-terminal amino acids. The mature form, which consists of 49% proline and 24% arginine, has been reported to inhibit phagocyte NADPH oxidase activity of pig neutrophils by binding to Src homology 3 (SH3) domains of $p47^{phox}$,[7] and to bind to and affect a SH3-containing signal transduction protein, $P130^{Cas}$.[8] Recently, a new function of PR-39 has been reported, i.e., inhibition of the ubiquitin-proteasome-dependent degradation of hypoxia-inducible factor-1α protein, resulting in accelerated formation of vascular structures *in vitro* and increased myocardial vasculature in mice.[5] As regards the mechanism of PR-39 function, Gao *et al.* demonstrated that PR-39 binds to the α7 subunit of the 26S proteasome and blocks degradation of NF-κB inhibitor IκBα via the ubiquitin-proteasome pathway without affecting overall proteasome activity.[9] From these observations, PR-39 seems to be a multifunctional polypeptide which can associate with key proteins, such as signaling molecules, in the cell.

Independently, PR-39 has been reported to induce the synthesis of syndecan-1, a transmembrane heparan sulfate proteoglycan involved in cell-to-matrix interactions and wound healing.[4] Previously, we revealed that the expression of syndecan-1 was reduced in human hepatocellular carcinomas with high metastatic potential and we speculated that syndecan-1 plays an important role in the inhibition of invasion and metastasis.[10] It is possible that modification of this process with PR-39 may provide a new strategy with which to inhibit invasion and metastasis. Therefore, we transduced the *PR-39* gene into human hepatocellular carcinoma cells and confirmed that PR-39 induced syndecan-1 expression and suppressed the invasive activity of the cells in a similar way to *syndecan-1* gene transduction.[6] Furthermore, the *PR-39* gene transduction altered the actin structure of the cells, while the *syndecan-1* gene transduction did not. In considering the mechanism of the actin structural alteration we focused on three previous observations. I) PR-39 has five repeats of the proline-rich motif, PXXPPXXP,[2] whose prototype is Sos, an activator of the ras guanine nucleotide exchange protein.[11] II) Proline-rich motifs have an ability to bind to SH3 domains.[12] III) PR-39 actually binds to SH3 domains of $p47^{phox}$ and $p130^{Cas}$.[7,8] Therefore, we hypothesized that the alteration of actin structure caused by PR-39 might

[1] These two individuals should be considered equivalent first authors.

[2] To whom requests for reprints should be addressed.
E-mail: yfujimot@asahikawa-med.ac.jp

result from the binding of the proline-rich region of PR-39 to the SH3 domain of protein(s) associated with the polymerization of actin filaments or intracellular signaling.

In the present study, we investigated the effects of PR-39 on the signal transduction pathways and tried to find the target molecules of PR-39 by using k-ras-transformed-NIH/3T3 fibroblasts[13, 14] which we further transfected with the *PR-39* gene tagged with hemagglutinin.

MATERIALS AND METHODS

Construction of *PR-39* gene vector A *PR-39* gene fragment (nucleotide 4–539) containing the whole coding region of pig *PR-39* gene[2] and a hemagglutinin (HA) epitope tag sequence at the C-terminus was amplified from pig small intestine mRNAs by RT-PCR (reverse transcriptase-polymerase chain reaction) using a primer (5′-GGGCTCAGGATTCACCAAAAGCTTTTAATGGGT-3′) for RT and two primers (5′-CTCACCTGGGCACCATG-GAG-3′, the RT primer) for PCR, and ligated into pT7Blue vector (Novagen, Inc., Madison, WI).[15] The PR-39 fragment in the pT7Blue vector was excised with *Eco*RI-*Xba*I, and ligated into pZeoSV2 expression vector (Invitrogen, San Diego, CA).

Cell culture and gene transfection Mouse fibroblast cells (NIH3T3 cells) provided by the Japanese Cancer Research Resources Bank (Tokyo) were maintained in Dulbecco's modified Eagle's medium (DMEM) supplemented with 10% fetal bovine serum, 2 m*M* L-glutamine, 100 units/ml penicillin, and 100 g/ml streptomycin sulfate. NIH/3T3 cells were transformed with human activated *k-ras* (Val12) gene (Ras cells) as we previously reported.[14] Ras cells were further transfected with the pZeoSV2 vector containing the *PR-39* gene (PR-39 cells). For the transfection of the *PR-39* gene, 40 μg of purified plasmid and 30 μg of Lipofectin (GIBCO-BRL, Gaithersburg, MO) were added to the Ras cells (approximately 50% confluent) in 100-mm culture dishes. After approximately 3-week selection with Zeocin (1000 μg/ml), three clones (PR-39A, PR-39B and PR-39C cells) were independently isolated from the three different dishes using cloning rings, and subcultured.

Staining of actin filament Cells grown on coverslips were rinsed twice with a cytoskeletal stabilizing buffer (4 *M* glycerol, 25 m*M* piperazine-N,N′-bis(2-ethanesulfonic acid) (PIPES) [pH 6.9], 1 m*M* EGTA, and 1 m*M* $MgCl_2$), incubated in the same buffer containing 0.2% Triton X-100 for 5 min at 20°C to extract soluble proteins, and fixed for 45 min at 20°C in 3.7% formaldehyde in phosphate-buffered saline (PBS). After two 10-min washes in PBS, cells were incubated with rhodamine-conjugated phalloidin (Amersham Corp., Tokyo) diluted 1:50 in PBS containing 0.5 mg/ml bovine serum albumin for 30 min. Cells were mounted with PermaFluor Aqueous Mountant (Shandon Corp., Pittsburg, PA), and observed using an Axioskop FL microscope (Carl Zeiss, Jena, Germany).

***In vitro* cell proliferation** Cell proliferation rates *in vitro* were determined by measuring the number of cells maintained with DMEM containing 10% fetal bovine serum (FBS) from days 1 to 4 after seeding onto 6-well tissue plates (2×10^3 cells/well). The number of cells was measured using a Coulter Cell Counter (Coulter Electronics Ltd., Luton, England).

Tumor growth in nude mouse Tumor growth rates *in vivo* were determined by measuring the tumor weight at 2 weeks after the subcutaneous inoculation of the cells (5×10^5 cells/mouse) into the right shoulder of male nude mice (5 weeks old) (Charles River Japan, Co., Atsugi). Animals were kept under laminar flow conditions with free access to food and water. All animals received humane care in compliance with the guidelines of Asahikawa Medical College.

Immunoprecipitation and western blot Cells were lysed in 50 m*M* N-(2-hydroxyethyl)piperazine-N′-2-ethanesulfonic acid (HEPES), pH 7.0, 150 m*M* NaCl, 10% (vol/vol) glycerol, 1% (vol/vol) Triton X-100, 1.5 m*M* $MgCl_2$, 1 m*M* EGTA plus proteinase inhibitor tablets (Seikagaku Kogyo, Tokyo). PR-39 or phosphatidylinositol 3-kinase p85α (PI3Kp85α) was immunoprecipitated from the cell lysates with anti-HA (Boehringer Mannheim, Tokyo) or anti-PI3Kp85α (Santa Cruz Biotechnology, Inc., Santa Cruz, CA) antibodies using protein A-Sepharose, respectively. After having been washed three times with lysis buffer, the antibody-antigen complexes were dissociated by heating at 100°C for 5 min in standard Laemmli sample buffer. The immunoprecipitated samples or 20 μg total proteins were separated on a 4–20% Tris-glycine gradient polyacrylamide gel (Bio-Rad Laboratories, Hercules, CA). Gels were electroblotted onto Immobilon (Millipore, Bedford, MA) or nitrocellulose membranes (Bio-Rad Laboratories), incubated with antibodies against HA, PI3Kp85α, ERK-1 and -2 (extracellular regulated kinases 1 and 2, Santa Cruz Biotechnology, Inc.), phospho-ERK 1 and 2 (Santa Cruz Biotechnology, Inc.), cyclin D1 (Santa Cruz Biotechnology, Inc.), Grb2 (Santa Cruz Biotechnology, Inc.), $p130^{Cas}$ (Santa Cruz Biotechnology, Inc.), or PLCγ (Santa Cruz Biotechnology, Inc.), horseradish-conjugated donkey anti-rabbit IgG (Seikagaku Kogyo) or donkey anti-mouse IgG (Seikagaku Kogyo). The immune complexes were detected with the ECL (enhanced chemiluminescence) detection system (Amersham International plc, Buckinghamshire, England). Silver staining of polyacrylamide gels was performed using a Silver Stain Kit (Bio-Rad Lab.).

Mitogen-activated protein kinase (MAPK) assay MAPK activity was determined using a p44/p42 MAP Kinase Assay Kit (New England BioLabs, Inc., Beverly, MA). Briefly, active MAPK was selectively immunoprecipitated from cell lysates using a monoclonal phospho-

antibody to p44/p42 MAPK. The resulting immunoprecipitate was then incubated with Elk-1 fusion protein in the presence of adenosine triphosphate (ATP) and kinase buffer; this allowed immunoprecipitated active MAPK to phosphorylate Elk-1. Phosphorylation of Elk-1 at Ser383 was measured by western blotting using a phospho-Elk-1 (Ser383) antibody.

c-Jun N-terminal kinase (JNK) assay JNK activity was determined using SAPK/JNK Kinase Assay Kit (New England BioLabs Inc.). Briefly, JNK was selectively pulled down from cell lysates using c-Jun fusion protein beads containing a high-affinity binding site for JNK. The beads were washed to remove nonspecifically bound proteins and then the kinase reaction was carried out in the presence of cold ATP. c-Jun phosphorylation was selectively measured using a phospho-c-Jun antibody.

PI3-kinase assay The cell lysates were prepared as described above for immunoprecipitation, and PI3-kinase was immunoprecipitated with the anti-p85α antibody. Immunocomplexes were collected on protein A-Sepharose beads, washed five times with lysis buffer and preincubated with 10 μl of 20 m*M* HEPES (pH 7.4), containing 2 mg/ml phosphatidylinositol (PI, Sigma Chemical Co., St. Louis, MO) on ice for 10 min. Kinase reaction was performed by the addition of 40 μl of reaction buffer (10 μCi of [γ-^{32}P]ATP, 20 m*M* HEPES, pH 7.4, 20 μ*M* ATP, 5 m*M* $MgCl_2$) at room temperature for 15 min. The reaction was stopped by the addition of 100 μl of 1 *M* HCl and extracted with 200 μl of 1:1 mixture of chloroform and methanol. The radiolabeled lipids were separated by thin-layer chromatography.[16] The conversion of PI to phosphatidylinositol 3-phosphate (PIP) was determined by autoradiography. PIP (10 μl of 0.5 mg/ml solution, BIOMOL Research Labs., Inc., Plymouth Meeting, PA) was used as a control for the position of the produced PIP on thin-layer chromatography after staining with iodine vapor. The radioactivity of the PIP was determined using a BAS2000 bioimaging analyzer (Fuji Film, Tokyo).

Statistical analysis Student's *t* test was used for statistical analysis of cell proliferation *in vivo*.

RESULTS

Expressions of ras and PR-39 in PR-39 cells by western blot analysis Expression levels of ras (Fig. 1A) and PR-39 (Fig. 1B) proteins were examined by western blot analysis. The NIH3T3 cells showed a very low expression of ras and no PR-39 expression. The Ras cells (NIH3T3 cells transformed with human activated *k-ras* gene) showed ras expression. The three clones, PR-39A, PR-39B and PR-39C, independently isolated after transduction of *PR-39* gene into Ras cells, expressed both ras and PR-39.

Alterations of morphology and actin structure As we had previously shown that *PR-39* gene transducion altered the morphology and actin structure of human hepatoma cells,[10] we initially examined the morphological change of the NIH3T3, Ras, PR-39A, PR-39B and PR-39C cells (Fig. 2). In phase-contrast microscopic examinations, the NIH3T3 cells showed a flat form. The Ras cells revealed a spindle shape with short or long spikes like filopodia. All of the PR-39A, PR-39B and PR-39C cells showed a flat form, like NIH3T3 cells (Fig. 2). The actin filaments were stained with rhodamine-conjugated phalloidin and subjected to immunofluorescence microscopy (Fig. 3). The NIH3T3 cells showed fine actin stress fibers oriented parallel to the long axes of the cells. The Ras cells showed short and faint actin filaments. The PR-39A, PR-39B and PR-39C cells revealed long and fine actin stress fibers, like the NIH3T3 cells (Fig. 3). These data show that the *PR-39* gene transduction into the Ras cells caused the morphology and actin structure to revert to those of NIH3T3 cells. These results strongly suggest that PR-39 might affect the signals associated with cytoskeletal actin structure, which was changed by *ras*-gene transfection.

Suppression of cell proliferation *in vitro* and *in vivo* We examined the cell proliferation rates of PR-39A, PR-39B and PR-39C cells *in vitro* and *in vivo* to investigate whether PR-39 affects the cell proliferation (Fig. 4). The cell proliferation rates *in vitro* were determined by measuring the number of cells after seeding onto 6-well tissue plates, using the cell counter. The numbers of NIH3T3, Ras, PR-39A, PR-39B and PR-39C cells were, respectively, 3.2, 9.6, 2.4, 3.9 and 2.2 fold at day 2; 6.9, 27.8, 8.1, 9.0 and 6.8 fold at day 3; and 16.8, 46.6, 21.6, 19.2 and 15.3 fold at day 4 compared with those at day 1 (Fig. 4A). The proliferation rate of the PR-39 cells was significantly decreased compared with that of the Ras cells at days 2, 3 and 4 ($P<0.05$), and almost the same as that of the NIH3T3 cells. The cell proliferation rate *in vivo* was determined from the tumor weight at 2 weeks after subcu-

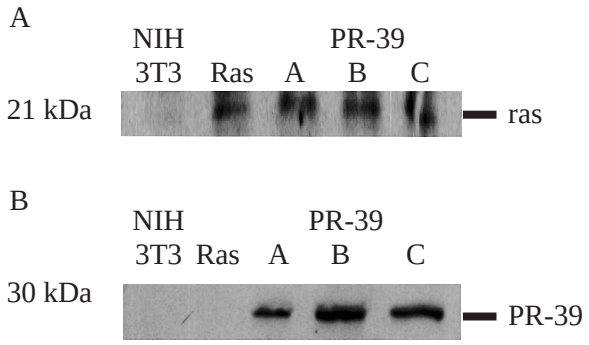

Fig. 1. Expressions of ras (A) and PR-39 (B) in PR-39 cells by western blot analysis. PR-39A, PR-39B and PR-39C cells showed both ras and PR-39 expressions, while ras cells showed only ras expression and NIH3T3 cells showed only a very low expression of ras.

taneous inoculation into nude mice. The NIH3T3 cells showed no tumors after inoculation, as far as could be determined. The mean tumor weights of the Ras, PR-39A, PR-39B and PR-39C cells were 3.1, 1.2, 1.3 and 1.0 g, respectively (Fig. 4B). The tumor weight of the PR-39 cells was significantly lower than that of the Ras cells ($P<0.005$). These data show that *PR-39* gene transduction suppressed cell proliferation both *in vitro* and *in vivo*, suggesting that PR-39 might affect the signals associated with mitogenesis.

Suppression of MAPK activity and cyclin D1 expression To understand the mechanism through which PR-39 suppressed the cell proliferation, we examined the cell signaling pathways involved in mitogenesis. We first examined the activity of MAPK, which is the main signal transduction protein for mitogenesis induced by activated ras.[17, 18] PR-39A, PR-39B and PR-39C cells showed almost the same proliferation rates both *in vitro* and *in vivo*, and therefore, we examined the MAPK activity of PR-39A cells as a representative. MAPK activity was

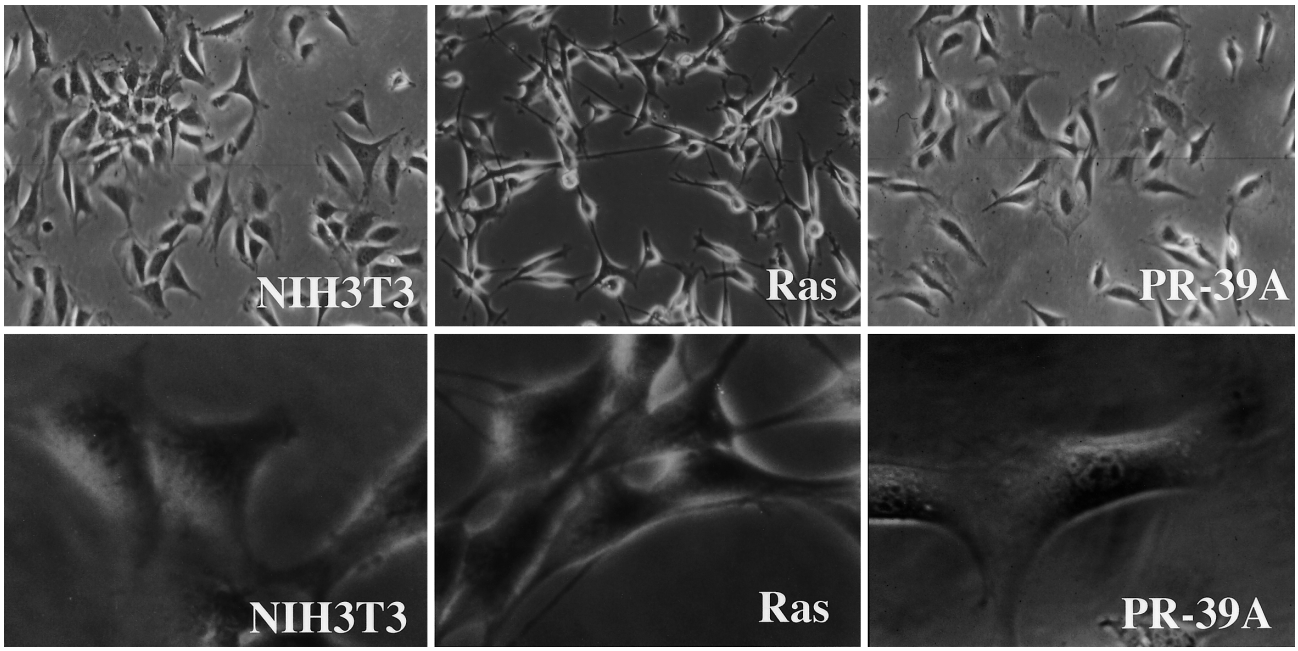

Fig. 2. Morphology of PR-39 cells. In phase-contrast microscopic examinations, NIH3T3 cells showed a flat form, while Ras cells revealed a spindle shape with short or long spikes like filopodia. However, PR-39A, PR-39B and PR-39C cells all showed a flat form like NIH3T3 cells. The morphology of PR-39A cells is shown as a representative. (×100 and ×1000)

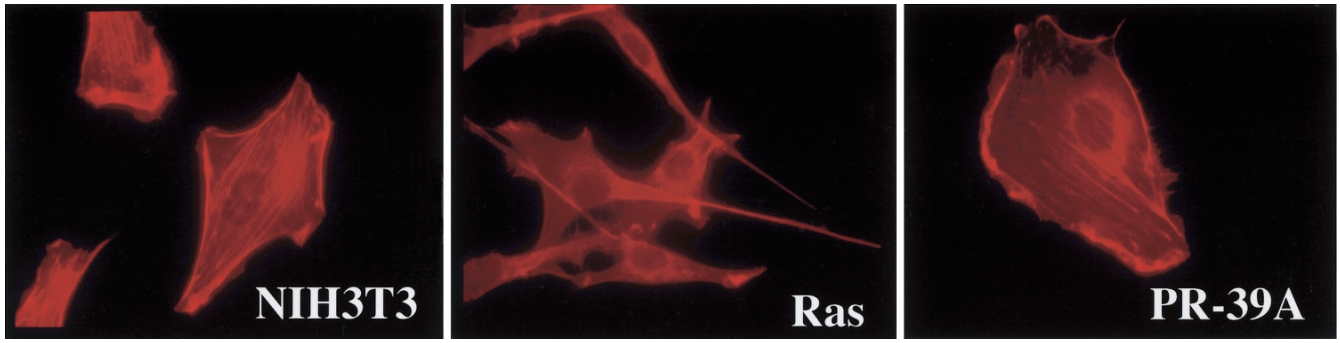

Fig. 3. Staining of actin filaments of PR-39 cells. Cells grown on coverslips were incubated with rhodamine-conjugated phalloidin and observed using immunofluorescence microscopy. NIH3T3 cells showed fine actin stress fibers oriented parallel to the long axes of the cells, while Ras cells showed short and faint actin filaments. However, PR-39A, PR-39B and PR-39C cells all revealed long and fine actin stress fibers like NIH3T3 cells. The actin structure of PR-39A cells is shown as a representative. (×1000)

determined in terms of the amount of Elk-1 phosphorylated by phospho-MAPK and the amount of phospho-MAPK. The MAPK activity of Ras cells was markedly high compared with NIH3T3 cells, but that of PR-39A cells was decreased compared with Ras cells (Fig. 5, A and B). On the other hand, the decrease of ERK-1 and ERK-2 expressions of PR-39A cells compared with those of Ras cells was only slight (Fig. 5C), suggesting that MAPK activity was decreased by PR-39 with a partial correlation with the protein amounts of ERK-1 and ERK-2 in Ras cells and PR-39A cells. We then examined the expression of cyclin D1, which exists downstream of MAPK and plays an important role in accelerating the cell cycle.[19, 20] The cyclin D1 expression of Ras cells examined by western blot analysis was markedly high compared with that of NIH3T3 cells, but that of PR-39A cells was decreased compared with Ras cells (Fig. 5C). These data suggest that PR-39 suppressed the cell proliferation by affecting the ras signal transduction and decreasing both MAPK activity and cyclin D1 expression.

Suppression of JNK activity We next examined the activity of JNK, which is also one of the effectors of ras, stimulating DNA synthesis by the phosphorylation of c-Jun via Rac and Raf pathways.[21] The JNK activity was determined in terms of the amount of phosphorylated c-Jun. The JNK activity of Ras cells was higher than that of NIH3T3 cells, but that of PR-39A cells was decreased compared with Ras cells (Fig. 6). These data suggest that PR-39 also decreases the JNK activity in addition to the MAPK activity, suggesting that PR-39 affects the JNK signaling pathway.

Binding of PR-39 to PI3Kp85α To explore the target molecule of PR-39 in activated-ras-mediated signal transduction in the cell, we tried to find PR-39 binding proteins in PR-39 cells by using co-immunoprecipitation analysis. As the *PR-39* gene was fused with the HA tag sequence at the C terminus, the cell lysates were subjected to co-immunoprecipitation with anti-HA antibody. The resulting precipitates were subjected to gradient polyacrylamide gel electrophoresis and the proteins were detected by silver staining. Several bands were detected only on PR-39A cells, in addition to mature and immature PR-39 at approximately 6 and 27 kDa, respectively (Fig. 7A). This result suggests that PR-39 binds to several proteins, some of which may be responsible for signal transduction in PR-39 cells. There might be several target molecules of PR-39 in the cell.

To identify the binding proteins of PR-39, the immunoprecipitates with anti-HA antibody were subjected to immunoblot analysis using four antibodies to signal transduction proteins containing an SH-3 domain which might be targets of the proline-rich motif of PR-39. Antibodies against Grb2, $p130^{Cas}$, PLCγ and PI3Kp85α were used because of molecular weight similarities to the recognized bands shown in Fig. 7A and their SH-3 domain-containing character. The antibodies against Grb2, $p130^{Cas}$ and PLCγ did not react with the bands detected in Fig. 7A (data not shown), suggesting that these proteins had no role in PR-39 binding. On the other hand, when an antibody to PI3Kp85α was used, a clear band was observed at approximately 85 kDa in the case of PR-39A cells (Fig. 7B). To examine the direct association of PR-39 with PI3Kp85α, cell lysates were subjected to immunoprecipitation with anti-PI3Kp85α antibody and the precipitates were sub-

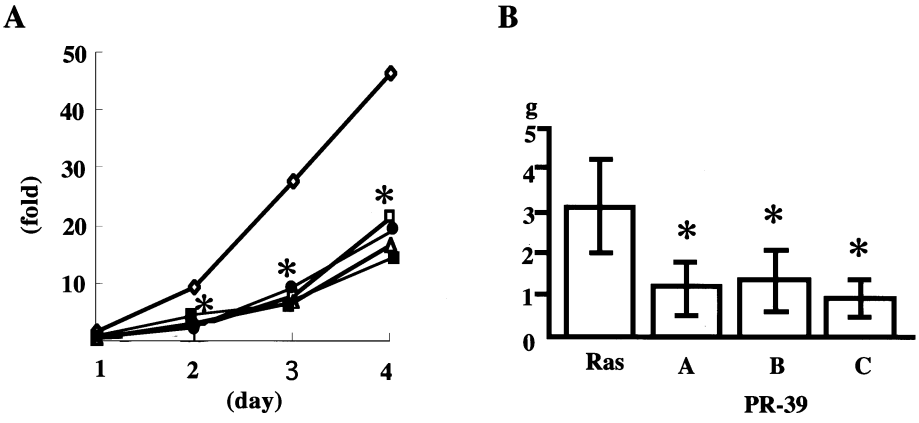

Fig. 4. Cell proliferation *in vitro* and *in vivo* of PR-39 cells. A, Cell proliferation rates *in vitro* were determined by measuring the number of cells from day 1 to day 4 after seeding onto 6-well tissue plates. The cell proliferation rates *in vitro* of PR-39A, PR-39B and PR-39C cells were significantly decreased to the level of NIH3T3 cells at days 2, 3 and 4 (∗ $P<0.05$). B, Cell proliferation rates *in vivo* were determined by measuring the tumor weight at 2 weeks after subcutaneous inoculation of the cells into nude mice. The proliferation rates *in vivo* of PR-39A, PR-39B and PR-39C cells were significantly decreased compared with that of Ras cells (∗ $P<0.005$), while NIH3T3 cells yielded no tumors. △ NIH3T3, ◇ Ras, □ PR-39A, ● PR-39B, ■ PR-39C.

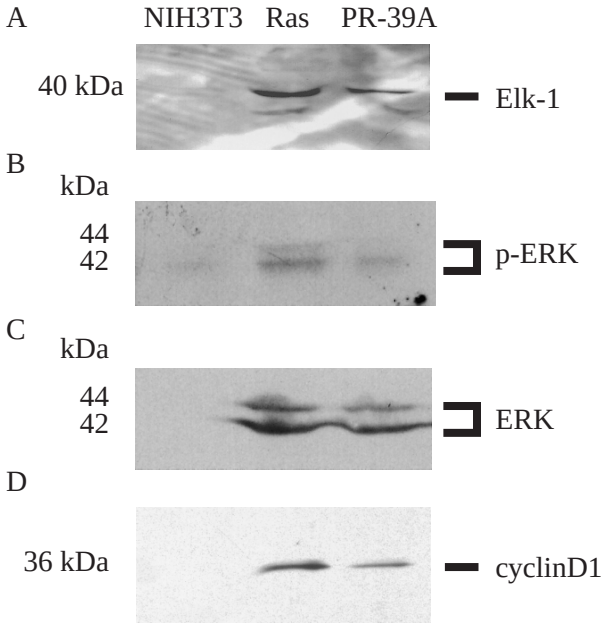

Fig. 5. MAP kinase activity and cyclin D1 expression of PR-39 cells. A, Active MAPK was selectively immunoprecipitated from cell lysates using an antibody to phospho-p44/p42 MAPK. The resulting immunoprecipitate was incubated with Elk-1 fusion protein to immunoprecipitate active MAPK with phosphorylated Elk-1. Phosphorylation of Elk-1 at Ser383 is measured by western blotting using a phospho-Elk-1 (Ser383) antibody. B, Western blot analysis of phospho-ERK was performed using anti-phospho-ERK antibody recognizing both phospho-ERK-1 and -2. C, Western blot analysis of ERK was performed using anti-ERK antibody recognizing both ERK-1 and -2. The MAPK activity of PR-39A cells was decreased compared with that of Ras cells, while ERK-1 and -2 expressions of PR-39 cells were slightly decreased compared with those of Ras cells. D, Western blot analysis of cyclin D1 was performed using anti-cyclin D1 antibody. The cyclin D1 expression of PR-39A cells was decreased compared to that of Ras cells.

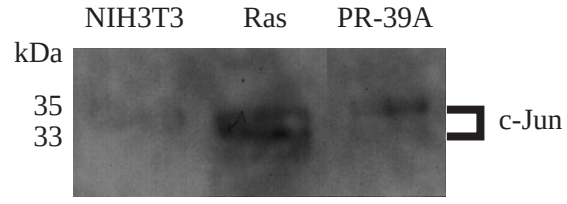

Fig. 6. JNK activity of PR-39 cells. JNK was selectively pulled down from cell lysates using c-Jun fusion protein and the kinase reaction was carried out in the presence of cold ATP. c-Jun phosphorylation was selectively measured using phospho-c-Jun antibody. The JNK activity of Ras cells was higher than that of NIH3T3 cells, but that of PR-39A cells was decreased compared with Ras cells.

jected to immunoblot analysis using anti-HA antibody. A clear band was observed at approximately 6 kDa, which is the size of mature-type PR-39 (Fig. 7C). These data demonstrate that the mature type of PR-39 binds to PI3Kp85α, suggesting that PI3Kp85α is one of the target molecules of PR-39 in the cell.

Suppression of PI3K activity To examine the effect of PR-39 binding on the function of PI3K, PI3K activity was determined in NIH3T3, Ras, PR-39A, PR-39B and PR-39C cells. The PI3K activity was measured in terms of the formation of the kinase product PIP and analyzed with a

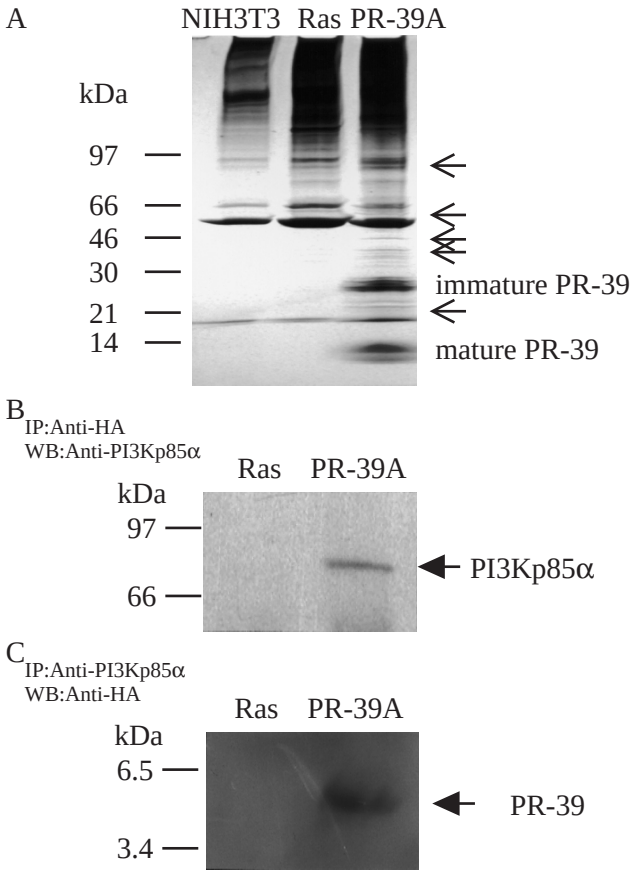

Fig. 7. Co-immunoprecipitation, silver staining and western blot analysis using anti-HA or anti-PI3Kp85α antibodies. A, The binding proteins of PR-39 were co-immunoprecipitated with anti-HA antibody. The precipitates were separated on a 4–20% gradient polyacrylamide gel and stained with silver. Several bands (arrows) were detected in addition to mature and immature PR-39. B, Cell lysates were immunoprecipitated with anti-HA antibody. The precipitates were immunoblotted with anti-PI3Kp85α antibody. A band was detected at approximately 85 kDa. C, Cell lysates were immunoprecipitated with anti-PI3Kp85α antibody. The precipitates were immunoblotted with anti-HA antibody. A band was detected at approximately 6 kDa. A mature type of PR-39 bound to PI3Kp85α.

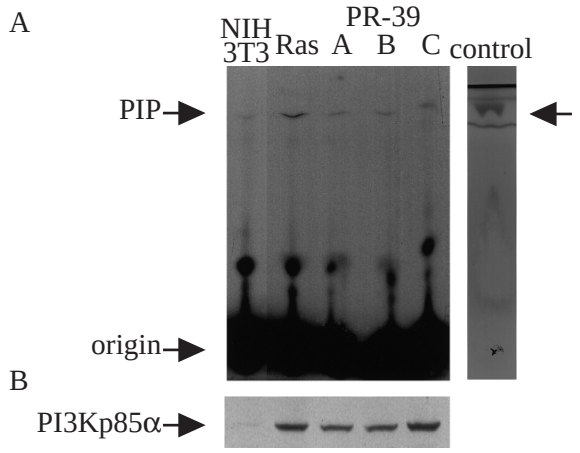

Fig. 8. PI3K activity and PI3Kp85α expression of PR-39 cells. A, Immunoprecipitates with anti-PI3Kp85α antibody from the cells were used to determine PI3K activity. The immunoprecipitates were incubated with PI in the presence of [γ-^{32}P]ATP. The production of radiolabeled PI 3-phosphate (PIP) was analyzed by thin-layer chromatography; the origin (O) of the chromatogram is indicated. PIP was used as a control for the position of the produced PIP. The PI3K activities of the PR-39A, PR-39B and PR-39C cells were lower than that of the Ras cells. B, PI3Kp85α expression was determined by western blot analysis using anti-PI3Kp85α antibody. The expressions of PI3Kp85α on PR-39A, PR-39B and PR-39C cells were almost the same as that on Ras cells.

BAS 2000 image analyzer. The relative radioactivities of PIP in NIH3T3, Ras and PR-39A, B, C cells were 288, 1724, 660, 645 and 610, respectively. The PI3K activity of Ras cells was approximately six times higher than that of NIH3T3 cells, but the activities of PR-39A, PR-39B and PR-39C cells were decreased to approximately 35−40% of that of Ras cells (Fig. 8A). However, the expression of PI3Kp85α in PR-39 cells was almost the same as that in Ras cells by western blot analysis (Fig. 8B). These data suggest that PR-39 might suppress the activity of PI3K by binding to the regulatory subunit, PI3Kp85α.

DISCUSSION

Activated k-ras protein, which is expressed in a high percentage of human malignant tumors such as lung, pancreatic and colonic carcinomas,[22] is a key molecule for mediating many signal transduction pathways associated with a variety of SH3-containing proteins in the cell.[13] The mature form of PR-39 consists of 49% proline and 24% arginine and is capable of binding to the SH3 domains of p47^{phox} and P130^{Cas}.[7, 8]

In the present study, we transfected *PR-39* gene into mouse NIH3T3 cells which had already been transformed with human activated *k-ras* gene and we found that *PR-39* gene transfectant showed reorganization of actin structure and suppression of cell proliferation both *in vitro* and *in vivo*. Furthermore, we found that PI3Kp85α, a regulatory subunit of PI3K, is one of the major target molecules of PR-39 in Ras cells. Taking these results together, it appears that PR-39 has an ability to revert Ras cells to the character of the parental NIH3T3 cells, and this phenomenon might be caused by the binding of PR-39 to PI3Kp85α in the cell.

Concerning the cytoskeletal change, PI3K is considered to be one of the effectors whose pathway involves the Rac, Cdc42 and Rho proteins. In addition, cell proliferation is mediated by augmented DNA synthesis through induction of transcription from the fos promoter through the MAPK pathway[23, 24] and from the c-Jun promoter through the JNK pathway,[25, 26] both of which pathways are also triggered by PI3K. Therefore, it is reasonable that the modulation of the PI3K activity by the binding of PR-39 affects the actin structure and the cell proliferation of Ras cells.

The present study revealed that the transduction of the *PR-39* gene into Ras cells resulted in re-assembly of actin stress fibers and disappearance of the filopodia. It is well known that the organization of actin structure is coordinately regulated by the Rho, Rac and Cdc42 GTPases.[13] Rho controls the assembly of actin stress fibers and focal adhesion complexes, Rac regulates actin filament accumulation at the plasma membrane to produce lamellipodia and membrane ruffles, and Cdc42 stimulates the formation of filopodia.[27] The transformation of NIH3T3 cells by activated ras induced actin filament accumulation at the plasma membrane and the formation of filopodia. However, the transduction of *PR-39* gene into Ras cells resulted in assembly of actin stress fibers and disappearance of the filopodia. These data demonstrate that ras stimulates Rac and Cdc42 and inhibits Rho, while PR-39 might inhibit Rac and Cdc42 and stimulate Rho by blocking ras signal transduction, including the PI3K pathway. Rac and Cdc42 selectively stimulate the JNK cascade leading to c-Jun transcriptional activity.[25, 26] The decreased JNK activity of PR-39 cells might support the suggestion that PR-39 inhibits the Rac and Cdc42 signaling pathways.

PI3K is composed of a regulatory p85 subunit and a catalytic p110 subunit, that, as an active complex, phosphorylates the 3-ring position of PI-4,5-bisphosphate to generate PI-3,4,5-triphosphate (PIP_3).[28] Downstream targets activated subsequent to PIP_3 include Akt/PKB, which has been implicated in inhibiting both apoptosis by the phosphorylation of Bad,[29] and the Raf-MEK-MAPK signaling pathway by the phosphorylation of Raf.[30] It is possible that the binding of PR-39 to PI3Kp85α affects the Akt/PBK pathway, resulting in a change of apoptotic rate or MAPK activity. Therefore, we examined the activity of Akt/PBK and the apoptotic rate of Ras and PR-39 cells, but no differences were observed between them (data not

shown), suggesting that PR-39 might not affect the Akt/PBK pathway in fibroblasts transformed by activated ras.

PR-39 seems to have an ability to revert Ras cells to the parental NIH3T3 character, because the cell morphology, actin structure and cell proliferation rate *in vitro* of PR-39 cells were almost the same as those of NIH3T3 cells. Furthermore, we demonstrated that the binding of the PR-39 to PI3Kp85α in the cell might cause this phenomenon. However, there are two observations that cannot be explained by the PR-39 binding to PI3Kp85α. One is that the proliferation rate *in vitro* of PR-39 cells was decreased to the level of NIH3T3 cells and the actin structure of PR-39 cells became very similar to that of NIH3T3 cells, but the PI3K, MAPK or JNK activity of PR-39 cells was not decreased to the level of NIH3T3 cells. The other is that the PR-39 cells still maintained the ability to form tumors in nude mice and retained loss of contact inhibition, unlike NIH3T3 cells (data not shown). These observations could be explained by either of two possibilities. One is that the decreased kinase activities were lower than some as-yet undetermined limit and could not maintain the ras phenotype except for tumorigenesis and the loss of contact inhibition.[31, 32] The other possibility is that the different signaling pathways associated with mitogenesis, the cytoskeleton or cell-cell communication were also affected by PR-39, in addition to the PI3K pathway. The latter possibility might be supported by the co-immunoprecipitation results shown in Fig. 7A; PR-39 binds to several proteins in addition to PI3Kp85α in PR-39 cells, although Grb2, $p130^{Cas}$ and PLCγ were not target molecules of PR-39 in this study.

With the advance in the molecular understanding of disease processes, it has been appreciated that many diseases, including cancers, result from malfunctions of signaling pathways.[33] Therefore, many researchers have focused their efforts upon seeking ways to manage disease through the manipulation of signal transduction pathways. It has been shown that inhibition of signal transduction pathways can be achieved by a variety of reagents including a Sos-derived peptidimer which blocks the Grb2-Sos signal[34] and MAPK-antisense RNA.[35] PI3K is also a potential target molecule for therapy of cancer. LY294002, which inhibits PI3K by competing with ATP for its substrate-binding site, induces specific G1 arrest in melanoma cells *in vitro*[36] and inhibits growth and ascites formation of ovarian carcinoma *in vivo*.[37] However, the high dose of LY294002 needed for a significant effect showed toxicity in the treated mice. In this study, *PR-39* gene transduction inhibited the cell growth of ras-transformed cells *in vitro* and *in vivo*, but showed no toxicity in tumor-inoculated mice (data not presented). Therefore, PR-39 could be an alternative candidate for antitumor therapy by modifying the signal transduction pathways in the cell.

ACKNOWLEDGMENTS

This research was supported by grants provided by the Ministry of Education, Science, Sports and Culture, Japan.

(Received February 14, 2001/Revised June 1, 2001/2nd Revised June 27, 2001/Accepted July 7, 2001)

REFERENCES

1) Agerberth, B., Lee, J.-Y., Bergman, T., Carlruist, M., Boman, H. G., Mutt, V. and Jornvall, H. Amino acid sequence of PR-39: isolation from pig intestine of a new member of the family of proline-arginine-rich antibacterial peptides. *Eur. J. Biochem.*, **202**, 849–854 (1991).
2) Storici, P. and Zanetti, M. A cDNA derived from pig bone marrow cells predicts a sequence identical to the intestinal antibacterial peptide PR-39. *Biochem. Biophys. Res. Commun.*, **196**, 1058–1065 (1993).
3) Boman, H. G. Peptide antibiotics and their role in innate immunity. *Annu. Rev. Immunol.*, **13**, 61–92 (1995).
4) Gallo, R. L., Ono, M., Povsic, T., Page, C., Eriksson, E., Klagsbrunl, M. and Bernfield, M. Syndecan, cell surface heparan sulfate proteoglycans, are induced by a proline-rich antimicrobial peptide from wounds. *Proc. Natl. Acad. Sci. USA*, **91**, 11035–11039 (1994).
5) Li, J., Post, M., Vokk, R., Gao, Y., Li, M., Metais, C., Sato, K., Tsai, J., Aird, W., Rosenberg, R. D., Hanpton, T. G., Ki, J., Sellke, F., Carmeriet, P. and Simons, M. PR-39, a peptide regulator of angiogenesis. *Nat. Med.*, **1**, 49–55 (2000).
6) Ohtake, T., Fujimoto, Y., Ikuta, K., Saito, H., Ohhira, M., Ono, M. and Kohgo, Y. Proline-rich antimicrobial peptide, PR-39 gene transduction altered invasive activity and actin structure in human hepatocellular carcinoma cells. *Br. J. Cancer*, **81**, 393–403 (1999).
7) Shi, J., Ross, C. R., Leto, T. L. and Blecha, F. PR-39, a proline-rich antibacterial peptide that inhibits phagocyte NADPH oxidase activity by binding to Src homology 3 domains of $p47^{phox}$. *Proc. Natl. Acad. Sci. USA*, **93**, 6014–6018 (1996).
8) Chan, Y. R. and Gallo, R. L. PR-39, a syndecan-inducing antimicrobial peptide, binds and affects $p130^{Cas}$. *J. Biol. Chem.*, **273**, 28978–28985 (1998).
9) Gao, Y., Lecker, S., Post, M. J., Hietaranta, A. J., Li, J., Volk, R., Li, M., Sato, K., Saluja, A. K., Steer, M. L., Goldberg, A. L. and Simons, M. Inhibition of ubiquitin-proteasome pathway-mediated IκBα degradation by a naturally occurring antibacterial peptide. *J. Clin. Invest.*, **106**, 439–448 (2000).
10) Matsumoto, A., Ono, M., Fujimoto, Y., Gallo, R. L., Bernfield, M. and Kohgo, Y. Reduced expression of syndecan-1 in human hepatocellular carcinoma with high metastatic potential. *Int. J. Cancer*, **74**, 482–491 (1997).

11) Yu, H., Chen, J. K., Feng, S., Dalgarno, D. C., Brauer, A. W. and Schreiber, S. L. Structural basis for the binding of proline-rich peptides to SH3 domains. *Cell*, **76**, 933–945 (1994).
12) Gout, I., Dhand, R., Hiles, I. D., Fry, M. J., Panayotou, G., Das, P., Truong, O., Totty, N. F., Hsuan, J., Booker, G. W., Campbell, I. D. and Waterfield, M. D. The GTPase dynamin binds to and is activated by a subset of SH3 domains. *Cell*, **75**, 25–36 (1993).
13) Malumber, M. and Pellicer, A. Ras pathways to cell cycle control and cell transformation. *Front. Biosci.*, **3**, D887–912 (1998).
14) Ura, H., Obara, T., Shudo, R., Itoh, A., Tanno, S., Fujii, T., Nishino, N. and Kougo, Y. Selective cytotoxicity of farnesylamine to pancreatic carcinoma cells and ki-ras-transformed fibroblast. *Mol. Carcinog.*, **21**, 93–99 (1998).
15) Storici, P. and Zanetti, M. A cDNA derived from pig bone marrow cells predicts a sequence identical to the intestinal antibacterial peptide PR-39. *Biochem. Biophys. Res. Commun.*, **196**, 1058–1065 (1993).
16) Chen, R.-H., Chang, M.-C., Su, Y.-H., Tsai, Y.-T. and Kio, M.-L. Interleukin-6 inhibits transforming growth factor-β-induced apoptosis through the phosphatidylinositol 3-kinase/Akt and signal transducers and activators of transcription 3 pathways. *J. Biol. Chem.*, **274**, 23013–23019 (1999).
17) Moodie, S. A., Willumsen, B. M., Weber, M. J. and Wolfman, A. Complexes of Ras.GTP with Raf-1 mitogen-activated protein kinase kinase. *Science*, **260**, 1658–1661 (1993).
18) Kyriakis, J. M., App, H., Zhang, X. F., Banerjee, P., Brautigan, D. L., Rapp, U. R. and Avruch, J. Raf-1 activates MAP kinase kinase. *Nature*, **358**, 417–421 (1992).
19) Lavoie, J. N., L'Allemain, G., Brunet, A., Miller, R. and Pouyssegur, J. Cycline D1 expressin is regulated positively by the p42/p44 MAPK and negatively by the p38/HOG MAPK pathway. *J. Biol. Chem.*, **271**, 20608–20616 (1996).
20) Winston, J. T., Coats, S. R., Wang, Y. Z. and Pledger, W. J. Regulation of the cell cycle machinery by oncogenic ras. *Oncogene*, **12**, 127–134 (1996).
21) McCarthy, S. A., Samuels, M. L., Pritchard, C. A., Abraham, J. A. and McMahon, M. Rapid induction of heparin-binding epidermal growth factor/diphtheria toxin receptor expression by Raf and Ras oncogenes. *Genes Dev.*, **15**, 1953–1964 (1995).
22) Bos, J. L. ras oncogenes in human cancer. *Cancer Res.*, **49**, 4682–4689 (1989).
23) Hu, Q., Klippel, A., Mulsin, A. J., Fantl, W. J. and Williams, L. T. Ras-dependent induction of cellular responses by constitutively active phosphatidylinositol-3 kinase. *Science*, **268**, 100–102 (1995).
24) Mcllory, J., Chen, D., Wjasow, C., Michaeli, T. and Backert, J. M. Specific activation of p85-p110 phosphatidylinositol 3-kinase stimulates DNA synthesis by ras- and p70 S6 kinase-dependent pathways. *Mol. Cell. Biol.*, **17**, 248–255 (1997).
25) Minden, A., Lin, A., Claret, F. X., Abo, A. and Karin, M. Selective activation of the JNK signaling cascade and c-Jun transcription activity by the small GTPases Rac and Cdc42Hs. *Cell*, **81**, 1147–1157 (1995).
26) Coso, O. A., Chiariello, M., Yu, J. C., Teramoto, H., Crespo, P., Xu, N., Miki, T. and Gutkind, J. S. The small GTP-binding proteins Rac1 and Cdc42 regulate the activity of the JNK/SAPK signaling pathway. *Cell*, **81**, 1137–1146 (1995).
27) Hall, A. Rho GTPases and actin cytoskeleton. *Science*, **279**, 509–514 (1998).
28) Tolias, K. F., Cantley, L. C. and Carpenter, C. L. Rho-family GTPases bind to phosphoinositide kinases. *J. Biol. Chem.*, **270**, 17656–17659 (1995).
29) Datta, S. R., Dudek, H., Tao, X., Masters, S., Fu, H., Gotoh, Y. and Greenberg, M. E. Akt phosphorylation of BAD couples survival signals to the cell-intrinsic death machinery. *Cell*, **91**, 231–241 (1997).
30) Rommel, C., Clarke, B. A., Zimmermann, S., Nunez, L., Rossman, R., Reid, K., Moelling, K., Yancopoulos, G. D. and Glass, D. J. Differentiation stage-specific inhibition of the Raf-EK-ERK pathway by Akt. *Science*, **286**, 1738–1741 (1999).
31) Hua, V. Y., Wang, W. K. and Duesberg, P. H. Dominant transformation by mutated human ras genes *in vitro* requires more than 100 times higher expression than is observed in cancers. *Proc. Natl. Acad. Sci. USA*, **94**, 9614–9619 (1997).
32) Nagy, J. I., Hossain, M. Z., Lynn, B. D., Curpen, G. E., Yang, S. and Turley, E. A. Increased connexin-43 and gap junctional communication correlate with altered phenotypic characteristics of cells overexpressing the receptor for hyaluronic acid-mediated motility. *Cell Growth Differ.*, **7**, 745–751 (1996).
33) Alexander, L. Targeting signal transduction for disease therapy. *Curr. Opin. Cell Biol.*, **8**, 239–244 (1996).
34) Cussac, D., Leprince, C., Liu, W., Cornill, F., Tiraboschi, G., Roques, B. P. and Garbay, C. A Sos-derived peptidimer blocks the Ras signaling pathway by binding both Grb2 SH3 domains and displays antiproliferative activity. *FASEB J.*, **13**, 31–39 (1999).
35) Nishio, K., Fukuoka, K., Fukumoyo, H., Sunami, T., Iwamoto, Y., Suzuku, T., Usuda, J. and Saijo, N. Mitogen-activated protein kinase antisense oligonucleotide inhibits the growth of human lung cancer cells. *Int. J. Oncol.*, **14**, 461–469 (1999).
36) Vlahos, C. J., Matter, W. F., Hui, K. Y. and Brown, R. F. A specific inhibitor of phosphatidylinositol 3-kinase, 2-(4-morpholinyl)-8-phenyl-4H-1-benzopyran-4-one (LY294002). *J. Biol. Chem.*, **269**, 5241–5248 (1994).
37) Hu, L., Zaloudek, C., Mills, G. B., Gray, J. and Jaffe, R. B. *In vitro* and *in vivo* ovarian carcinoma growth inhibition by a phosphatidylinositol 3-kinase inhibitor (LY294002). *Clin. Cancer Res.*, **6**, 880–886 (2000).